ALMA Observations of the DART Mission: Characterizing the Impact Ejecta at Sub-Millimeter Wavelengths with ALMA

Nathan X. Roth[1,2], Stefanie Milam[1], Anthony Remijan[3], Martin Cordiner[1,2], Michael W. Busch[4], Cristina Thomas[5], Andrew Rivkin[6], Arielle Moullet[3], Ted Roush[7], Jian-Yang Li[8], and Mark Siebert[9]

[1]NASA Goddard Space Flight Center, MD, USA [2]Catholic University of America, Washington, DC, USA [3]National Radio Astronomy Observatory, VA, USA [4]SETI Institute, CA, USA [5]Northern Arizona University, AZ, USA [6]Johns Hopkins Applied Physics Laboratory, MD, USA [7]NASA Ames Research Center, CA, USA [8]Planetary Science Institute, AZ, USA [9]University of Virginia, VA, USA

Introduction

- The DART mission provided the first test of the kinetic impactor planetary defense technique, targeting the Didymos-Dimorphos binary asteroid and impacting at UT 23:14 2022 September 26.
- We conducted pre-impact and post-impact observations toward Didymos-Dimorphos with the Atacama Large Millimeter Array (ALMA).

Observations

- We conducted pre-impact observations on September 15 to provide a baseline continuum measurement of Didymos-Dimorphos and to characterize Didymos' spectral emissivity.
- We conducted post-impact observations with ALMA and the Atacama Compact Array (ACA) from approximately 3-9 hours post-impact.
- All observations (executions) utilized the Band 7 receiver centered near 345 GHz (0.87 mm).
- The spatial resolution of ALMA and the ACA were 50 km and 200 km, respectively, at the distance of the asteroids, so neither was spatially resolved.

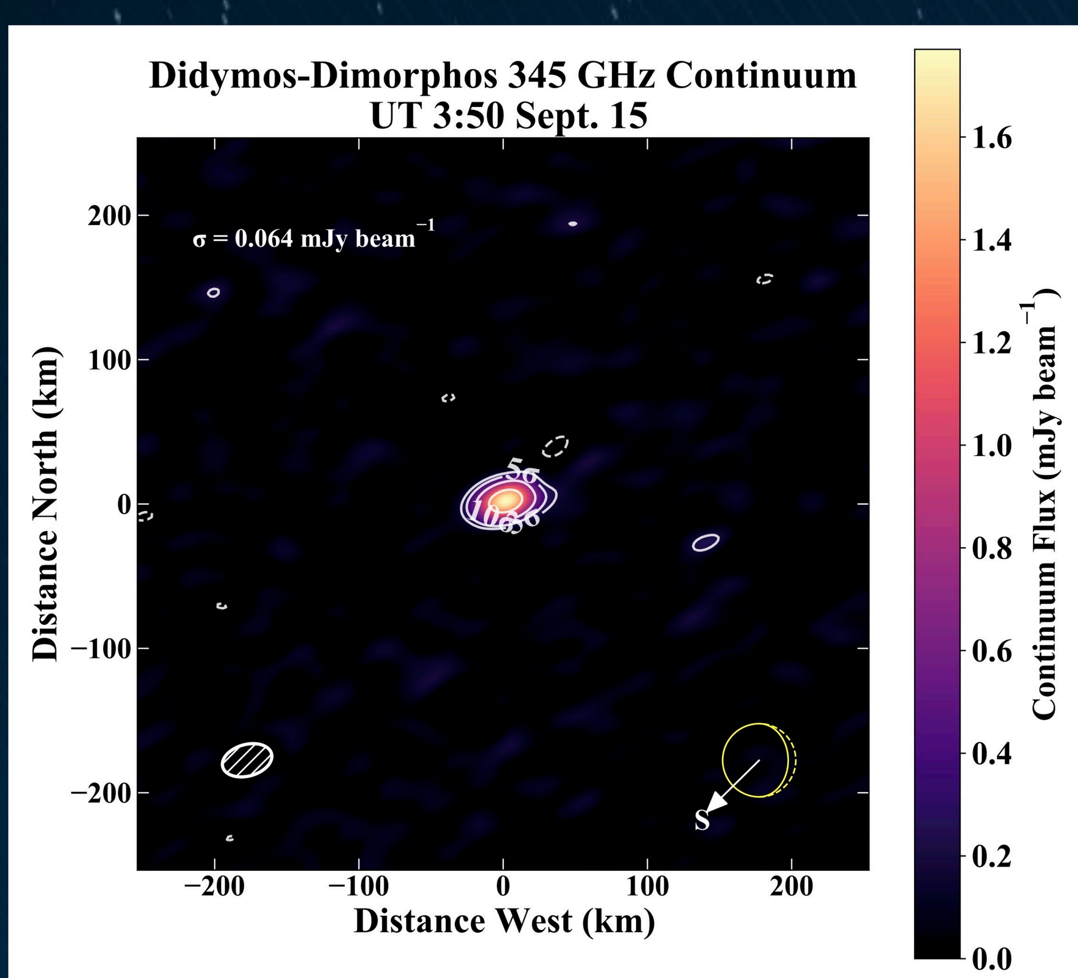

Figure 1. Pre-impact ALMA image of Didymos-Dimorphos. The 1σ image RMS is indicated in the upper right, the hatched ellipse in the lower left is the synthesized beam size, and an illumination diagram indicates the direction of the Sun (S). Contours are increments of the image RMS.

Didymos' Spectral Emissivity

- We utilized our pre-impact measurements to obtain a baseline continuum flux and characterize the millimeter spectral emissivity of Didymos. Figure 1 shows our pre-impact ALMA image of the asteroids.
- We calculated the spectral emissivity, ε, of Didymos following Altenhoff et al. (2004).
- For Didymos' flux density of 1.53 ± 0.14 mJy, we calculate ε = 0.87 ± 0.08. This emissivity is consistent with ε of the handful of other siliceous and carbonaceous asteroids measured at mm wavelengths (e.g., ALMA Partnership 2015, Chichura et al. 2022) with values on the order of unity.
- This likely reflects the silicate-dominated nature of Didymos (de León et al. 2010, Dunn et al. 2013).

Post-Impact Continuum Fluxes

- Our post-impact observations sampled continuum emission at λ = 0.87 mm from the asteroids and ejecta
- Using the pre-impact emissivity, we calculated the flux density attributable to Didymos on the impact date as 2.60 mJy and 0.11 mJy for Dimorphos. Hence, Didymos and the ejecta dominated our measurements. Sample images are shown in Figures 2 and 3.
- We calculated the integrated flux density in our post-impact images within the region where S/N > 3. Our results are shown in Figure 4 for the 12 m array.
- We subtracted Didymos' flux to isolate that of the ejecta. Our results are given in Table 1.

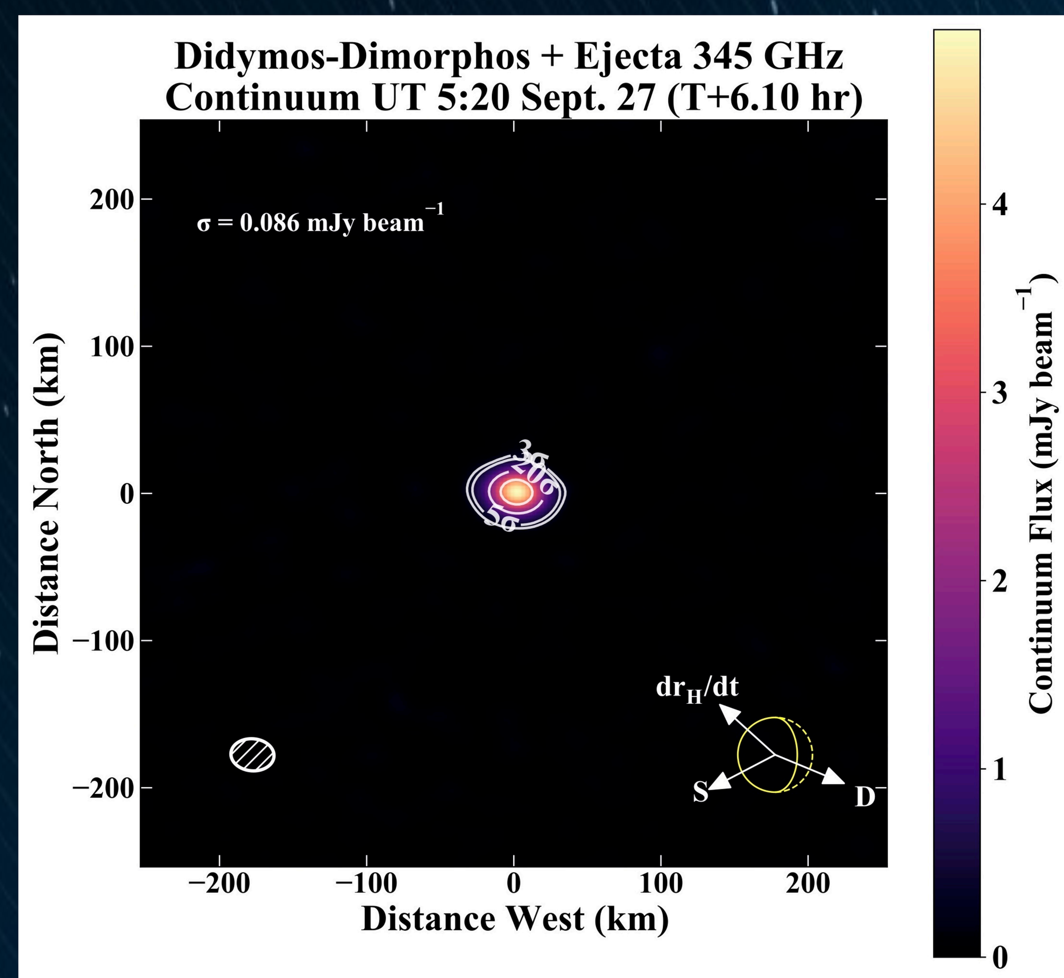

Figure 2. Post-impact ALMA image of Didymos-Dimorphos plus the ejecta, with traces and labels as in Figure 1. The direction of the DART spacecraft impact (D) and the heliocentric velocity vector have been added.

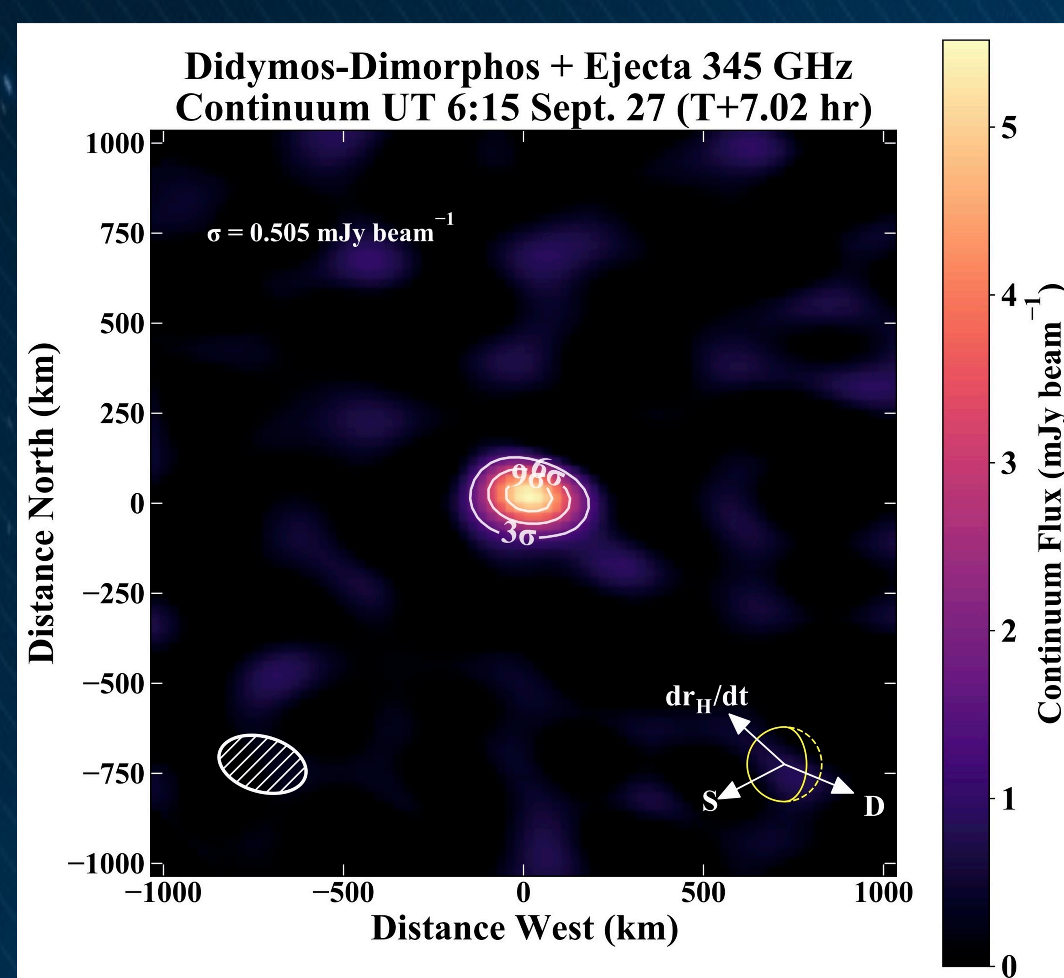

Figure 3. Post-impact ACA image of Didymos-Dimorphos plus the ejecta, with traces and labels as in Figure 2.

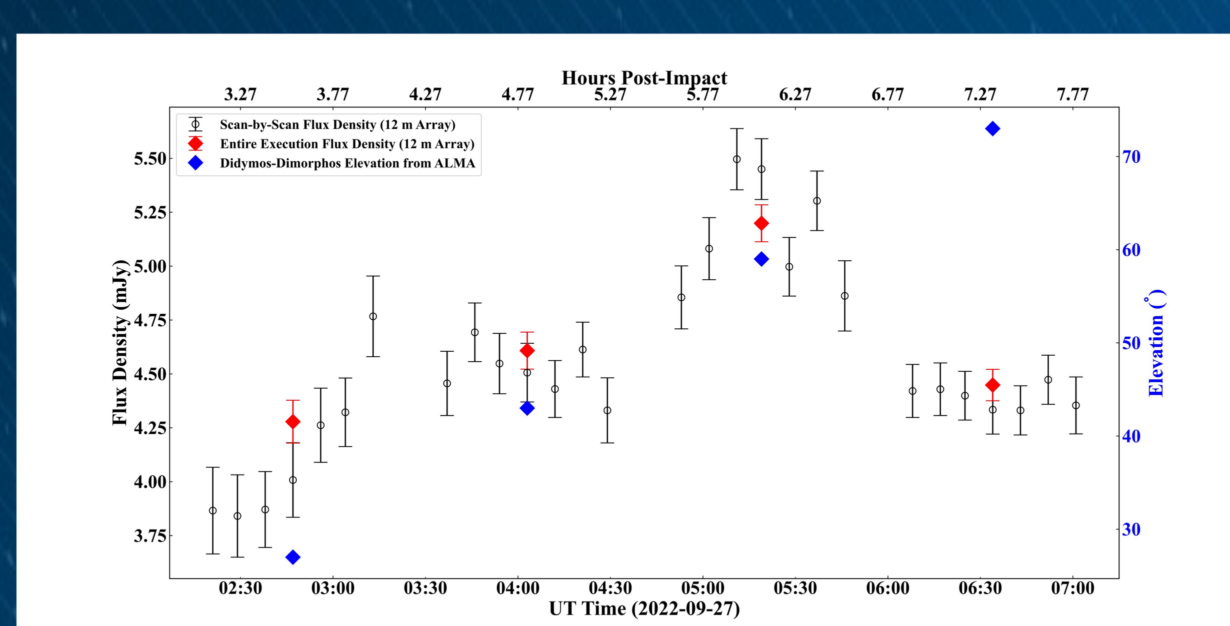

Figure 4. Post-impact fluxes measured for Didymos-Dimorphos and the ejecta with the 12 m array. Fluxes are shown on a scan-by-scan basis (black) and when imaging all scans in an execution simultaneously (red). Fluxes are integrated within the region where S/N > 3, approximately 50 km in radius from the asteroids (Figure 2). The elevation at the midpoint of each 12 m array execution is indicated (blue).

References

- Altenhoff, W. J. et al. 2004, A&A, 415, 771
- Jewitt, D. & Lu, J. 1990, ApJ, 365, 738
- Boissier, J. et al. 2012, A&A, 542, A73
- Tsuchiyama, A. et al. 2011, Science, 333, 1125
- Daly, R. T. et al. 2023, Nature, https://doi.org/10.1038/s41586-023-05810-5
- Li, J-Y. et al. 2023, Nature, https://doi.org/10.1038/s41586-023-05811-4
- Graykowsky, A. et al. 2023, Nature, https://doi.org/10.1038/s41586-023-05852-9
- de León, J. et al. 2010, A&A, 517, A23
- Dunn, T. et al. 2013, Icarus, 222, 273

Acknowledgments

This work was supported by the Planetary Science Division Internal Scientist Funding Program through the Fundamental Laboratory Research (FLaRe) work package (N.X.R., S.N.M., M.A.C., S.B.C.), as well as the NASA Astrobiology Institute through the Goddard Center for Astrobiology (proposal 13-13NAI7-0032; S.N.M., M.A.C., S.B.C.). It makes use of the following ALMA data: ADS/JAO.ALMA #2021.A.00013.S. ALMA is a partnership of ESO (representing its member states), NSF (USA), and NINS (Japan), together with NRC (Canada), MOST and ASIAA (Taiwan), and KASI (Republic of Korea) in cooperation with the Republic of Chile. The Joint ALMA Observatory is operated by ESO, AUI/NRAO, and NAOJ. The National Radio Astronomy Observatory is a facility of the National Science Foundation operated under cooperative agreement by Associated Universities, Inc.

Post Impact Ejecta Masses

- We calculated dust masses for each ALMA observation following the methods of Jewitt & Luu (1990) and Boissier et al. (2012). The dust mass (M) is related to the measured flux density (S_λ) by the dust opacity κ_λ as $S_\lambda = \frac{2kTM\kappa_\lambda}{\lambda^2\Delta^2}$, where k is the Boltzmann constant and Δ the geocentric distance.
- The dust opacity depends on the optical properties of the material. Optical constants at λ = 0.87 mm are not available for ordinary chondrites, which are likely most representative of S-type asteroid material (Tsuchiyama et al. 2011).
- We considered four materials to estimate the range of optical properties for ordinary chondrites based on the available optical constants in the literature: pure crystalline olivine, pure amorphous olivine, pure amorphous pyroxene, and a mixture of 2/3 amorphous pyroxene to 1/3 amorphous olivine (Figure 5).
- We calculated the range of dust masses for these materials, which range from 6×10^6 – 7×10^7 kg depending on the material and assuming the differential particle size distribution measured with HST (Li et al. 2023).
- Using an average value for all our executions, we obtain a range of masses from (1-5)x10^7 kg, representing 0.2-1.2% of Dimorphos' total mass (Daly et al. 2023). Our results are shown in Table 1.

Discussion

- Our calculated ejecta masses are consistent with Graykowski et al. (2023), who estimated ejecta masses of 0.3-0.5% of Dimorphos' mass based on optical wavelength observations.
- The measured fluxes increase until plateauing during the third execution of the 12 m array (T+6 hours) followed by a decrease in the fourth execution. This may be due to sub-millimeter sized particles exiting the ALMA maximum recoverable scale and may constrain the speed of these grains.

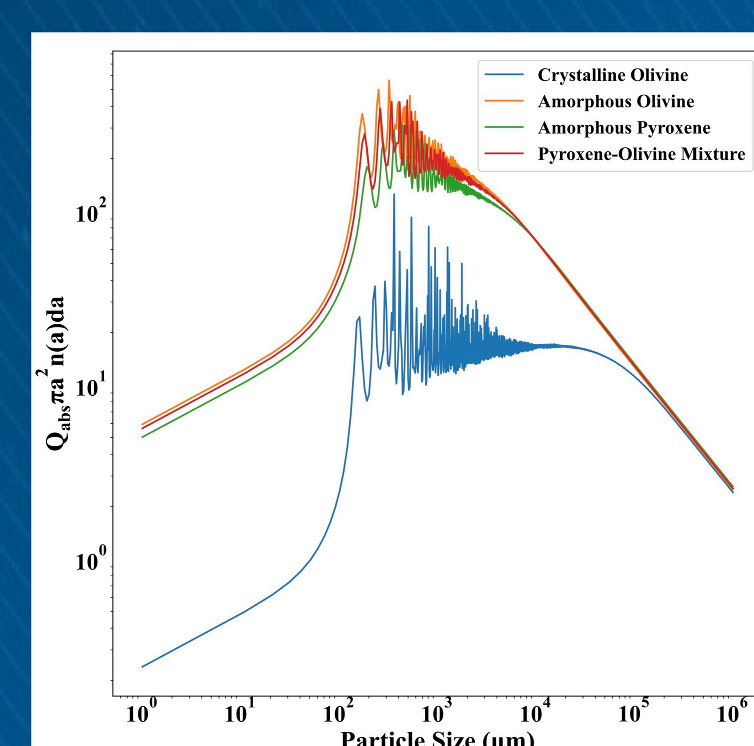

Figure 5. Absorption cross-sections for the material mixtures considered to approximate optical properties of the ejecta assuming a particle distribution $n(a) \propto a^{-2.7}$, where a is the particle radius. Our ALMA measurements are most sensitive to sub-millimeter size particles.

Table 1. Ejecta Flux Densities and Mass Estimates

Time$^{(a)}$	Total Flux$^{(b)}$	Ejecta Flux^{c}	Ejecta Mass (10^7 kg)$^{(d)}$			
(Post-Impact)	(mJy)	(mJy)	Cry-Oli	Amo-Oli	Amo-Pyr	Pyr-Oli Mix
3.52†	4.3 ± 0.4	1.7 ± 0.4	4.48	0.91	0.99	0.93
3.77‡	3.0 ±0.8	<2.4 (3σ)	<6.39	<1.29	<1.41	<1.33$^{(e)}$
4.77†	4.6 ± 0.4	2.0 ± 0.4	5.37	1.08	1.18	1.11
5.27‡	4.6 ± 0.7	2.0 ± 0.7	5.22	1.05	1.15	1.08
6.10†	5.2 ± 0.4	2.6 ± 0.5	6.94	1.40	1.53	1.44
7.02‡	4.3 ± 0.6	1.7 ± 0.6	4.44	0.90	0.98	0.92
7.27†	4.5 ± 0.4	1.9 ± 0.4	4.94	0.99	1.09	1.02
8.60‡	3.8 ± 0.6	1.2 ± 0.6	3.22	0.65	0.71	0.67
Weighted Average$^{(f)}$	4.6 ± 0.2	1.8 ± 0.2	5.01	1.01	1.10	1.04

NOTE—$^{(a)}$Time post-impact (hours). ^{b}Flux density for Didymos plus the ejecta integrated across the region where the intensity > 3σ. Uncertainties include image RMS plus an 8% uncertainty in absolute flux calibration. ^{c}Flux density after subtracting the 2.60 mJy flux density of Didymos. Uncertainties include an additional 10% to account for the subtraction of Didymos' calculated flux. ^{d}Dust mass calculated following the methods of (Jewitt & Luu 1990; Boissier et al. 2012) as outlined in Section 3.4. Masses are given assuming grain compositions of (pure crystalline olivine, pure amorphous olivine, pure amorphous pyroxene, 2/3 amorphous pyroxene to 1/3 amorphous olivine). Dust mass uncertainties are directly proportional to those for the calculated ejecta flux. $^{(e)}$3σ upper limit on ejecta dust mass. †12 m execution. $^{(f)}$Weighted average of all flux measurements (excluding the 3σ upper limit from the first ACA execution). ‡ACA execution.